

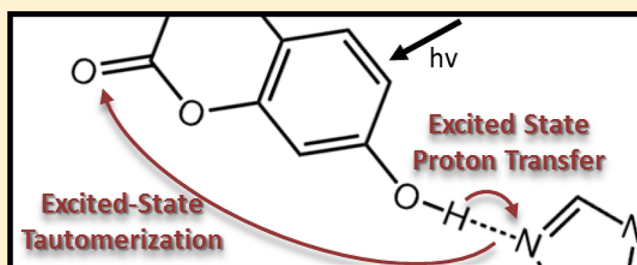
Base-Induced Phototautomerization in 7-Hydroxy-4-(trifluoromethyl)coumarin

Brittany C. Westlake,[†] Jared J. Paul,[‡] Stephanie E. Bettis,[†] Shaun D. Hampton,[†] Brian P. Mehl,[†] Thomas J. Meyer,^{*,†} and John M. Papanikolas^{*,†}

[†]Department of Chemistry, University of North Carolina at Chapel Hill, Chapel Hill, North Carolina 27599-3290, United States

[‡]Department of Chemistry, Villanova University, Villanova, Pennsylvania 19085, United States

ABSTRACT: Excited-state proton-transfer dynamics between 7-hydroxy-4-(trifluoromethyl)coumarin and 1-methylimidazole base in toluene were studied using ultrafast pump–probe and time-resolved emission methods. Charge-transfer excitation of the hydroxycoumarin shifts electron density from the hydroxyl group to the carbonyl, resulting in an excited state where proton transfer to the base is highly favored. In addition to its photoacid characteristics, the shift in the hydroxycoumarin electronic distribution gives it characteristics of a photobase as well. The result is a tautomerization process occurring on the picosecond time scale in which the 1-methylimidazole base acts as a proton-transfer shuttle from the hydroxyl group to the carbonyl.



1. INTRODUCTION

Proton-coupled electron-transfer (PCET) reactions and half reactions in which both an electron and proton are transferred have been widely studied.^{1–8} They play a special role in biology and in energy conversion reactions in chemistry. The mechanistic details of how PCET reactions occur have been elucidated in considerable detail.^{1,8} Clearly defined pathways have been identified in which proton transfer is followed by electron transfer (PT–ET) and in which electron transfer is followed by proton transfer (ET–PT). Although more complex microscopically, pathways have also been identified in which concerted electron–proton transfer (EPT) occurs simultaneously. The combined motion of protons and electrons are also observed in excited states, where intramolecular excitations result in changes in electron density that, for example, can enhance the acidity of a dissociable proton.⁷ This effect provides the basis for excited-state proton transfer (ESPT).^{9,10}

ESPT occurs in a class of molecules that can undergo dramatic increases in pK_a upon electronic excitation.¹¹ Enhanced acidity accompanying changes in electronic structure dramatically influence reaction dynamics of proton-transfer events. On the basis of the Förster equation, eq 1, intramolecular charge transfer (ICT) excitation can result in increased acidities of up to 6–8 pK_a units.¹¹ As an example, excited 2-naphthol demonstrates an increase in acidity of 6.6 pK_a units for the phenolic proton when compared to the ground state.¹² In the Förster equation, $h\nu_1$ is the absorbance energy maxima of the protonated excited state, and $h\nu_2$ is the absorbance energy maxima for the corresponding deprotonated form.

$$pK_a^* = pK_a - \left[\frac{h\nu_1 - h\nu_2}{2.3RT} \right] \quad (1)$$

Time scales for proton transfer are of importance in potential applications. For example, in most applications, an ideal photoacid in water should have a ground-state pK_a of 8 and a $pK_a^* < 2$, below $pK_a(H_3O^+) = -1.74$, and deprotonates in a few nanoseconds following electronic excitation in aqueous solution, followed by slow reprotonation.¹¹ The converse of superacids, superbases, has also been observed in excited states in which charge-transfer excitation creates a basic site. Chen et al. found evidence for superbase formation following excitation of an arginine amide-containing peptide where the amide becomes a superbase following electronic excitation.¹³ For molecules that contain preformed intramolecular hydrogen bonds without a requirement for diffusion, proton transfer is more readily in competition with excited-state decay.

Coumarins are highly emissive compounds that are commonly utilized as laser dyes. In particular, 7-hydroxycoumarin derivatives have well-characterized emission spectra and have been investigated for their ESPT properties.^{14,15} Three emitting states have been observed for these types of compounds, Figure 1. One is the weakly emitting acid that is observable in

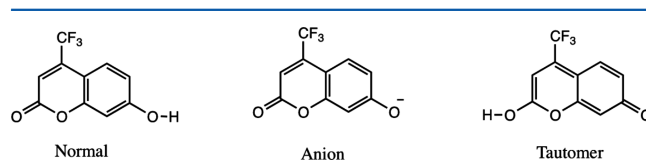


Figure 1. Emitting forms of 7-hydroxy-4-(trifluoromethyl)coumarin (CouOH).

Received: August 27, 2012

Revised: November 21, 2012

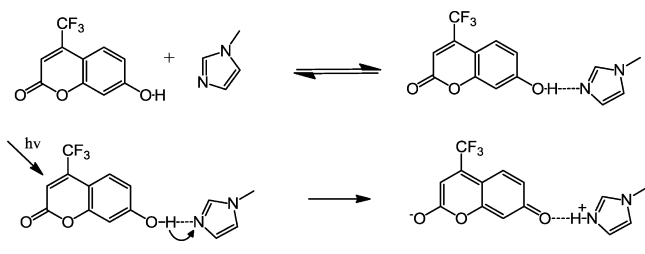
Published: November 28, 2012



non-hydrogen-bonding, low dielectric solvents, such as chloroform.¹⁴ The other two emissions are significantly enhanced and occur at lower energy. They occur from the deprotonated anion and from a tautomer emission that is reached by proton transfer to the carbonyl group of the chromophore. The tautomer form becomes favored in the excited state because ICT excitation of 7-hydroxycoumarin derivatives (CouOH) shift electron density from the hydroxyl group to the carbonyl, leading to an electronic configuration in which proton transfer to the carbonyl is favored. A key for tautomer formation is a proton-transfer solvent, such as water, which can donate a proton to the carbonyl in the excited state.¹⁶

Ultrafast transient techniques have been used to investigate ESPT to the solvent.^{17,18} We recently reported a photo-induced electron–proton transfer (photo-EPT) process in the 4-hydroxy-4'-nitro-biphenyl molecule in which instantaneous, concerted proton transfer in the excited state occurs to an external H-bonded base. It was noted that this was due to instantaneous formation of an excited state with an elongated proton–base bond and not a violation of the Franck–Condon principle.¹⁹ A similar conclusion was reached for the ESPT mechanism following excitation of the hydrogen-bonded adduct formed between 7-hydroxy-4-(trifluoromethyl)coumarin and 1-methylimidazole (Scheme 1) in the nonpolar, non-hydrogen-bonding solvent

Scheme 1



toluene with proton transfer to the external base 1-methylimidazole being highly favored.

Here, we expand on the earlier work with 7-hydroxy-4-(trifluoromethyl)coumarin to examine the excited-state dynamics that occur subsequent to the initial ultrafast proton-transfer event. In its excited state, the coumarin dye is not only a photoacid, but the shift in electron density toward the carbonyl group causes it to also act as an intramolecular excited-state photobase.

We apply time-resolved absorption and emission measurements to reveal a novel tautomerization in which an intramolecular proton translation of the proton occurs kinetically induced by H-bonding to a second base molecule.

2. EXPERIMENTAL SECTION

A. Materials and Preparation. 7-Hydroxy-4-(trifluoromethyl)-1-coumarin (CouOH) (98%), 1-methylimidazole (1-MeIm) (99%), and toluene (Chromasolv Plus for HPLC, >99.9%) were all purchased from Sigma-Aldrich and used as received. Solutions for femtosecond transient absorption and time-correlated single-photon counting (TCSPC) were prepared with 0.34 mM CouOH and 2 mM 1-MeIm base in toluene. Solutions for UV–vis and steady-state emission measurements were made at a range of base concentrations. Prior to time-resolved emission measurements, the samples were deaerated by bubbling argon gas through the sample for ~30 min.

B. UV–Vis. UV–vis absorption measurements were carried out by using an Agilent Technologies Model 8453 diode array spectrophotometer. Initial absorption measurements were conducted in a 1 cm cuvette and then repeated in a 2 mm cuvette to recreate the path length and concentration conditions used in the femtosecond transient absorption measurements.

C. Steady-State Emission. Steady-state emission measurements were obtained by using a PTI QuantaMaster emission spectrometer. Samples were excited with 355 nm light, and the sample emission was scanned from 360 to 700 nm with background correction. Emission collected using the 2 mm cuvette required that it be placed at a 45° angle relative to the excitation and emission collection slits in the spectrometer. Slit widths of 0.35 mm were used. For steady-state emission studies carried out at 77 K, samples were prepared in an NMR tube, degassed for 30 min with argon gas, and cooled using liquid nitrogen in a home-built dewar that was placed directly in the spectrometer.

D. Time-Correlated Single-Photon Counting (TCSPC). The apparatus consists of a frequency-doubled, mode-locked Ti:Sapphire laser, with a repetition rate adjusted by an acousto-optic modulator (AOM) used in a single-pass configuration. The femtosecond pulses selected by the AOM excite the sample, and the emitted light is collected at 90° relative to excitation, focused onto the slit of a 240 mm focal length single-grating monochromator, and delivered to a cooled, multichannel plate photomultiplier tube (MCP, Hamamatsu R3809U-51). The signal from the MCP is amplified, sent into a 200 MHz constant fraction discriminator (CFD, Tennelec 454), and then used as the start pulse for a time-to-amplitude converter (TAC, Tennelec 864). The stop pulse is obtained by focusing 10% of the excitation beam onto a Si:PIN photodiode, whose output is sent into a variable delay box, then to a CFD, and finally to the TAC. The TAC's output is sent to a multichannel analyzer that is interfaced to a PC. The instrument response of the apparatus is 80 ps at the full width at half-maximum (fwhm).

Femtosecond transient absorption measurements were conducted by using a pump–probe technique that has been described previously in detail.^{19,20} Briefly, the excitation source is a chirped pulse Ti:Sapphire regenerative amplification laser system (Clark CPA 2001) that outputs a 800 mW, 775 nm pulse at a 1 kHz rep rate, with an autocorrelation fwhm of 250 fs. The probe pulse was generated by focusing a small portion of the beam into a CaF₂ window to generate a white light continuum from 380 to 700 nm. The spot size at the sample was ~280 μm. The 355 nm pump pulse was created with a tunable Clark optical parametric amplifier (OPA) (1420 nm) followed by second-harmonic generation (710 nm) and fourth-harmonic generation (355 nm) by focusing the respective beams through beta barium borate (BBO) crystals. The data were collected at the magic angle polarization (54.7 degrees) with the pump beam focused to a ~1400 μm spot size and power of 0.60 mW. Samples with concentrations of 0.34 mM CouOH with 2 mM 1-MeIm base were prepared. Samples were placed in a 2 mm quartz cuvette and degassed with argon gas for 30 min prior to data collection. The chirp in the white light was accounted for by using an optical gating technique described elsewhere.^{19,20}

3. RESULTS AND DISCUSSION

A. Steady-State Spectroscopy. Absorption Spectroscopy. The ground-state UV–visible spectrum of 7-hydroxy-4-(trifluoromethyl)coumarin (CouOH) in toluene is centered at 330 nm when no base is present (Figure 2). This band arises from an intramolecular charge transfer (ICT) transition that

shifts electron density from the phenolic group to the carbonyl. The addition of 1-methylimidazole as a base (:B) results in the systematic shift of the absorption maximum from 330 to 342 nm, consistent with ground-state hydrogen bond formation. The relative similarity in the pK_a values for hydroxycoumarin ($-\text{OH}$, 7.26) and 1-methylimidazole (N ; 7.4) implies formation of a short, tight H-bond.²¹ Benesi–Hildebrand analysis of the spectral shifts observed with a series of base concentrations between 0.01 and 2000 mM (Figure 2) gave a hydrogen-bonding association constant (K_a) in the ground state of 2100 M^{-1} .²²

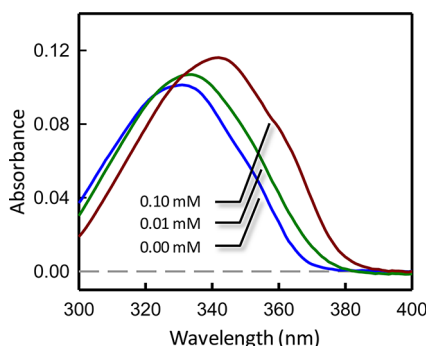


Figure 2. Ground-state UV-vis absorption spectra for 0.34 mM hydroxycoumarin with 0 (blue line), 0.01 (green line), and 0.1 mM (red line) 1-methylimidazole in toluene. The red shift in the absorption band with increasing base reflects the increase in the formation of the hydrogen-bonded adduct.

Emission Spectroscopy. When excited at 330 nm with no base, hydroxycoumarin emits weakly at 403 nm. Addition of small amounts (0.01 mM) of base to the solution dramatically increases the emission intensity (Figure 3), yielding an emission

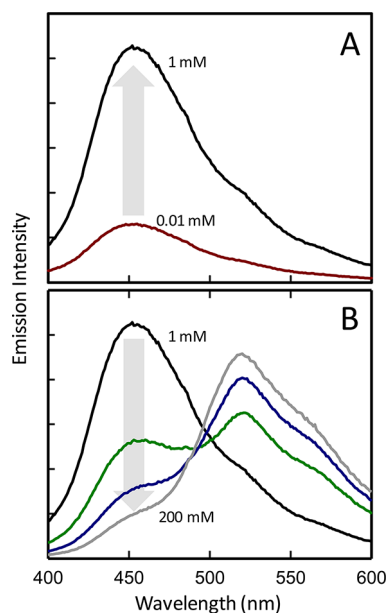


Figure 3. Room-temperature steady-state emission data for 0.34 mM hydroxycoumarin in toluene with varying amounts of 1-methylimidazole; excitation at 355 nm. (A) Low base concentrations of 0.01 (red) and 1 mM (black). The increase in emission intensity reflects the increase in concentration of the hydrogen-bonded adduct. (B) High base concentrations of 1 (black), 40 (green), 100 (blue), and 200 mM (gray).

band with $\lambda_{\text{max}} = 460 \text{ nm}$, whose intensity systematically increases upon continued addition of base up to 1 mM. In agreement with other studies, we have assigned the 460 nm band to emission from a configuration in which the proton is transferred to the base but remains hydrogen bonded to the hydroxycoumarin anion, that is, $(\text{CouO}^- \cdots \text{H}^+ - \text{B})^*$.^{23–25} Complete removal of the proton by a strong base shows the hydroxycoumarin anion to be strongly emissive and further red-shifted with $\lambda_{\text{max}} = 506 \text{ nm}$. Adduct emission can be viewed as arising from an anion, whose ground state is stabilized by a H-bond interaction with the protonated base. The dramatic increase in emission of the hydrogen-bonded adduct, even at low base concentrations, highlights the importance of the hydrogen bond between the base and hydroxycoumarin and its effect on the molecule's fluorescence properties. Similar observations were made by Moriya and co-workers where coumarin solutions with added water or alcohol enabled hydrogen bonding.^{16,26,27}

Steady-state emission spectra at higher base concentrations (10–200 mM) are shown in Figure 3B. With continually higher base concentrations, the emission band at 460 nm decays, while a new band grows in at 520 nm. On the basis of previous reports, the band at longer wavelengths is assigned to the hydroxycoumarin tautomer where the proton is associated with the carbonyl group at the other end of the molecule.^{16,26–28} Studies by Moriya described a water bridge in a similar 7-hydroxycoumarin system that enabled the site of protonation to be transferred from the photoacidic OH group to the photo-basic carbonyl.¹⁶ In the case of the hydroxycoumarin with 1-methylimidazole in toluene, there are no extra protons to be transferred, and formation of the tautomer necessitates the translation of the proton from one side of the coumarin to the other or between excited coumarin–base couples.

The emission spectra observed in a low-temperature toluene glass at 77 K (Figure 4) show a 440 nm band upon the addition

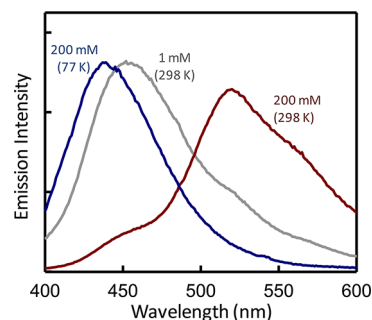


Figure 4. Steady-state emission data for 0.34 mM hydroxycoumarin with 200 mM 1-methylimidazole at 77 K (blue). Also shown are the room-temperature emission data with 1 (gray) and 200 mM (red) 1-methylimidazole. Samples were excited at 355 nm.

of 1-methylimidazole at concentrations that yield tautomer emission at room temperature. The blue shift relative to the fluid solution is due to a lack of solvent reorganization in the rigid environment in the excited-state charge distribution. The absence of tautomer emission indicates a suppression of the mechanism for delivering the proton to the carbonyl oxygen in the frozen state and at the same time implies that tautomer formation occurs in the excited state after photon absorption occurs.

B. Time-Resolved Spectroscopy. The observation of emission from the H-bonded CouOH points to rapid proton transfer accompanying excitation of the ICT transition in CouOH , at least on a time scale that is short compared to the excited-state lifetime.

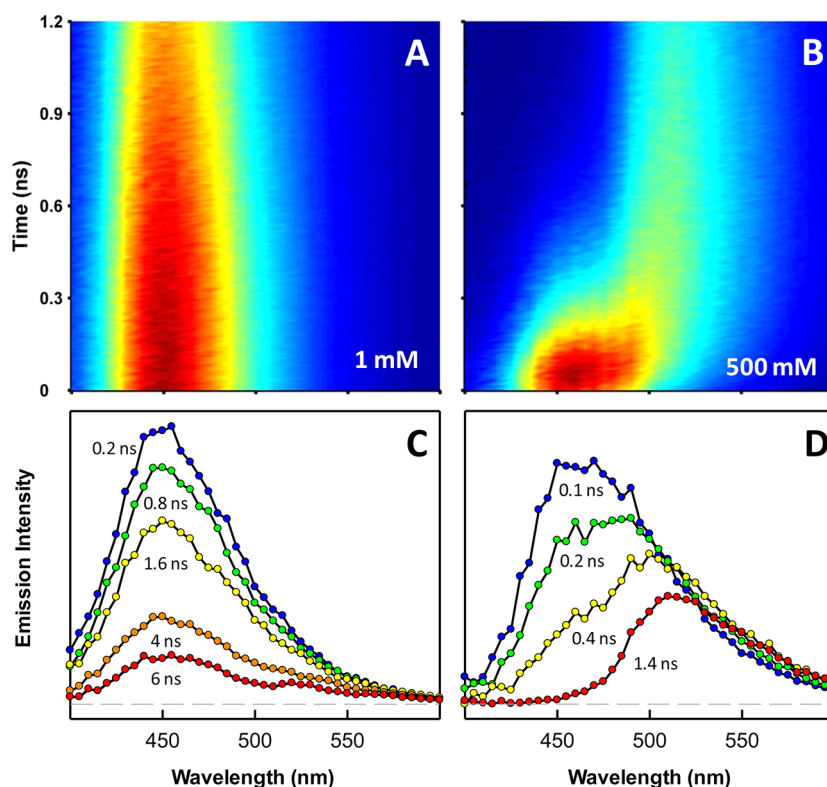


Figure 5. (A) TCSPC emission spectra for hydroxycoumarin with low base concentration (1 mM), following 360 nm excitation. (B) TCSPC emission spectra for hydroxycoumarin with excess base concentration (500 mM), following 360 nm excitation. (C) TCSPC emission spectra for hydroxycoumarin with low base concentration (1 mM), following 360 nm excitation obtained at 0.2, 0.8, 1.6, 4, and 6 ns. (D) TCSPC emission spectra for hydroxycoumarin with excess base concentration (500 mM), following 360 nm excitation obtained at 0.1, 0.2, 0.4, and 1.4 ns.

A recent report from our group examined these early time dynamics using a combination of transient absorption and coherent Raman methods.¹⁹ The results of that work pointed to a novel photo-EPT process in which the proton is transferred to the base during the photoexcitation process, resulting in a hydroxycoumarin anion that is hydrogen bonded to a protonated methylimidazole base. Here, we focus on the dynamics that take place following that initial proton-transfer event on longer time scales.

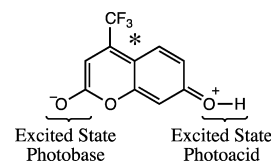
Transient Emission. Shown in Figure 5 is time-resolved emission data for hydroxycoumarin with low (2 mM) and high (500 mM) concentrations of added base following 360 nm excitation by an ultrafast laser pulse. Data were collected at a series of emission wavelengths, and Figure 5A and B shows intensity maps that depict the emission as both a function of detection wavelength and time. Emission spectra at a given time are obtained by taking horizontal slices through the data set. Spectra at a series of times are shown for the two base concentrations in Figure 5C and D.

For the low base concentration, the spectra observed at early times (200 ps) show a band at 459 nm that uniformly decays with a 3 ns lifetime. The spectrum agrees well with the steady-state emission spectrum observed under similar conditions and is attributed to the hydroxycoumarin anion hydrogen bound to the protonated base, that is, $\text{CouO}^- \cdots \text{H}^+ - \text{B}$.

A more complicated spectral time profile is seen in the time-resolved emission data collected from hydroxycoumarin in the presence of high base concentrations. At early times, the spectrum appears with a band at 459 nm, and during the first 200–300 ps, the band red shifts to 520 nm, resembling the time-integrated spectrum. The spectral shift of the emission from

459 to 520 nm represents changes to the hydroxycoumarin emission as the protonated base is shuttled from the photoacidic side of the molecule to the photobasic side (Scheme 2),

Scheme 2



providing a direct view of the tautomerization process. The time-dependent spectral shift is also direct evidence that the tautomerization occurs in the excited state and that the base-dependent emission spectra (Figure 4) are not simply the result of ground-state equilibrium.

Femtosecond Pump–Probe. Femtosecond transient absorption spectra obtained utilizing a 355 nm excitation pulse and white light continuum probe extending from 400 to 650 nm are shown in Figure 6 for both low base and high base concentrations. At early times, the spectra show a narrow positive-going feature with $\lambda_{\text{max}} \approx 400$ nm and a broad negative-going feature centered at 465 nm. The negative-going feature is not a ground-state bleach (hydroxycoumarin does not absorb in this spectral region) but rather stimulated emission from the photoexcited state.

The stimulated emission at 465 nm is shown as a function of pump–probe delay for the low base concentration in Figure 7. A significant fraction ($\sim 75\%$) of the stimulated emission appears within the time resolution of our instrument (~ 800 fs),

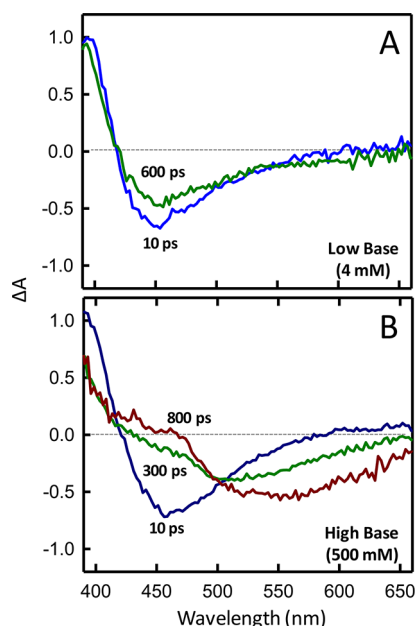


Figure 6. (A) Femtosecond transient absorption difference spectra for HFC with low base concentration (4 mM) or the 1:1 adduct, following 355 nm excitation obtained at 10 (blue line) and 600 ps (green line). (B) Femtosecond transient absorption difference spectra for hydroxycoumarin with high base concentration (500 mM), following 355 nm excitation obtained at 10 (blue line), 300 (green line), and 800 (red line). These spectra show the changes to stimulated emission as the molecule undergoes tautomerization.

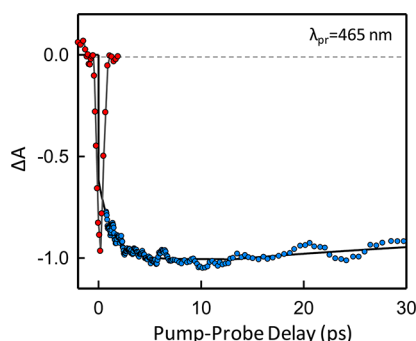


Figure 7. Femtosecond transient stimulated emission data for the hydroxycoumarin 1:1 adduct with 1-MeIm (2 mM) in toluene following 355 nm excitation and detected in a transient differential transmission mode. The red points in the figure represent the instrument response (IR) of the experiment. The IR shown is 800 fs, which is larger than the usual IR of the experiment of 250 fs. This increase in IR is due to an interaction with the pump beam. The pump excitation beam induces a nuclear response in the toluene, represented in the graph. Blue points represent the experimental data at 465 nm, and only data points outside of the instrument response are shown.

followed by a delayed growth during the first 5–10 ps after photoexcitation. The growth of this band reflects the appearance of the strongly emissive $(\text{CouO}^-\cdots\text{H}^+-\text{B})^*$ species. The prompt emission is attributed to an ultrafast photo-EPT process.¹⁹ The delayed growth in the stimulated emission intensity suggests that a subset of the ensemble undergoes delayed proton transfer to the hydrogen-bonded base, perhaps due to a distribution of different configurations at the moment of photon absorption.

The dynamical shift in the emission is also observed in the pump–probe spectra obtained with high base concentrations. Figure 8 shows pump–probe transients monitored at 465 and

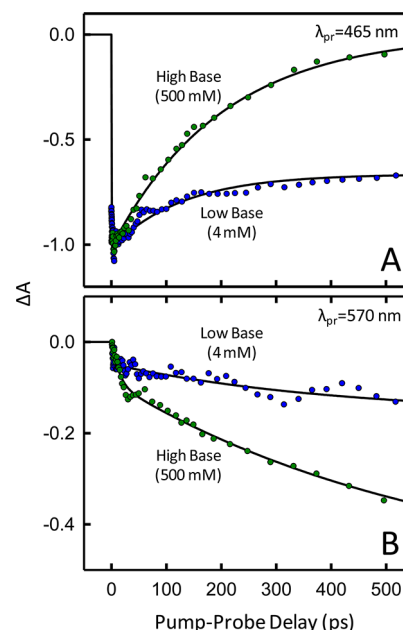


Figure 8. Femtosecond pump–probe kinetics of hydroxycoumarin under high base (500 mM) and low base (4 mM) concentrations for probe detection wavelengths of (A) 465 and (B) 570 nm.

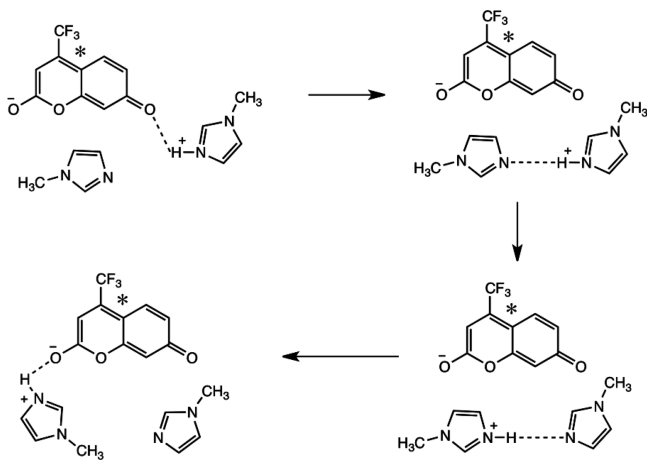
570 nm for two different base concentrations. The transient spectrum at early time (10 ps) is the same for low and high base concentrations. On a time scale of 100s of picoseconds, the decay of the band at 465 nm occurs concurrently with the growth of a band at 570 nm, which is attributed to the green emission of the tautomer.

The kinetics associated with tautomerization depend on the base concentration. For the lower base concentration, there is a decay of only 15–20% of the total pump–probe signal at 465 nm during the first 800 ps after photoexcitation and a slight increase in signal at 570 nm. At this concentration, ~90% of the hydroxycoumarin is present as a hydrogen-bonded adduct, yet a relatively small fraction of the systems undergo tautomerization. This is in contrast to the kinetics observed with 500 mM added base, where a complete loss of the 465 nm signal and significant growth at 570 nm is observed during this same time period.

This dependence on base concentration indicates that the mechanism for shuttling the proton from one side of the hydroxycoumarin to the other involves more than one base molecule. In aqueous solutions, it has been suggested that this occurs via a hydrogen-bonding bridge formed by a chain of water molecules.^{16,27} In this configuration, the proton that leaves the photoacid site need not be the same proton that appears at the photobase side. Because 1-methylimidazole does not contain an acidic proton and the solvent is toluene, a hydrogen-bonding network does not exist, and the proton that is eventually shuttled to the photobase must come from the hydroxyl group.

The involvement of more than one base suggests that proton shuttling is not simply by diffusion of the protonated base. A possible mechanism, consistent with the observed base dependence, is illustrated in Scheme 3. In that mechanism, proton shuttling occurs by formation of the proton adduct, $\text{MeIm}\cdots^+\text{HImMe}$, which

Scheme 3



“shuttles” the proton to the more basic Cou–O[−] site on the dye through a configuration in which the proton “hops” from one methylimidazole to another in close proximity.

4. CONCLUSIONS

We report here the ESPT dynamics between 7-hydroxy-4-(trifluoromethyl)coumarin and 1-methylimidazole base in toluene. The toluene solvent is nonpolar and lacks the ability to act as a proton-transfer medium without utilizing the 1-methylimidazole as a shuttle. Protonated hydroxycoumarin is a weak emitter; however, ICT in hydroxycoumarin upon electronic excitation results in an excited state where proton transfer to base is highly favored. The deprotonated anion emits intensely. In addition to its characteristics as a photoacid, the ICT event in hydroxycoumarin shifts the electronic distribution in the molecule to give it characteristics of a photobase as well. The carbonyl component becomes more electron rich, and a tautomerization event is favored provided a mechanism for proton delivery is in place. In a fluid state, the 1-methylimidazole base can act as a proton-transfer shuttle and favor tautomerization at higher base concentrations. However, in the frozen state at 77 K, the mobile delivery system is shut off, and only emission from the anion at 439 nm is observed with no tautomer emission. The excited-state dynamics of proton transfer are also base-concentration-dependent. In all cases, proton transfer occurs rapidly, with a majority of the events taking place within the time resolution of the experiment. At higher base concentrations, the tautomer emission grows in over the course of 100s of picoseconds as the proton is shuttled to the photobasic site in the hydroxycoumarin from the mobile 1-methylimidazole base.

AUTHOR INFORMATION

Corresponding Author

*E-mail: john_papanikolas@unc.edu (J.M.P.); tjmeyer@unc.edu (T.J.M.).

Notes

The authors declare no competing financial interest.

ACKNOWLEDGMENTS

Support from the National Science Foundation through Grants CHE-0957215 (T.J.M.) and CHE-0809045 and later CHE-1213379 (J.M.P.) is gratefully acknowledged.

REFERENCES

- (1) Weinberg, D. R.; Gagliardi, C. J.; Hull, J. F.; Murphy, C. F.; Kent, C. A.; Westlake, B. C.; Paul, A.; Ess, D. H.; McCafferty, D. G.; Meyer, T. J. *Chem. Rev.* **2012**, *112*, 4016–4093.
- (2) Meyer, T. J.; Huynh, M. H. V.; Thorp, H. H. *Angew. Chem., Int. Ed.* **2007**, *46*, 5284–5304.
- (3) Huynh, M. H. V.; Meyer, T. J. *Chem. Rev.* **2007**, *107*, 5004–5064.
- (4) Cukier, R. I.; Nocera, D. G. *Annu. Rev. Phys. Chem.* **1998**, *49*, 337–369.
- (5) Reece, S. Y.; Nocera, D. G. *Annu. Rev. Biochem.* **2007**, *78*, 673–699.
- (6) Mayer, J. M. *Annu. Rev. Phys. Chem.* **2004**, *55*, 363–390.
- (7) Tolbert, L. M.; Solntsev, K. M. *Acc. Chem. Res.* **2002**, *35*, 19–27.
- (8) Gagliardi, C. J.; Vannucci, A. K.; Concepcion, J. J.; Chen, Z.; Meyer, T. J. *Energy Environ. Sci.* **2012**, *5*, 7704–7717.
- (9) Hsieh, C.-C.; Jiang, C.-M.; Chou, P.-T. *Acc. Chem. Res.* **2010**, *43*, 1364–1374.
- (10) Gagliardi, C. J.; Westlake, B. C.; Kent, C. A.; Paul, J. J.; Papanikolas, J. M.; Meyer, T. J. *Coord. Chem. Rev.* **2010**, *254*, 2459–2471.
- (11) Nunes, R. M. D.; Pineiro, M.; Arnaut, L. G. *J. Am. Chem. Soc.* **2009**, *131*, 9456–9462.
- (12) Tolbert, L. M.; Haubrich, J. E. *J. Am. Chem. Soc.* **1994**, *116*, 10593–10600.
- (13) Chen, X.; Turecek, F. *J. Am. Chem. Soc.* **2006**, *128*, 12520–12530.
- (14) Yakatan, G. J.; Juneau, R. J.; Schulman, S. G. *Anal. Chem.* **1972**, *44*, 1044–1046.
- (15) Zinsli, P. E. *J. Photochem.* **1974/75**, *3*, 55–69.
- (16) Moriya, T. *Bull. Chem. Soc. Jpn.* **1983**, *56*, 6–14.
- (17) Rini, M.; Magnes, B.-Z.; Pines, E.; Nibbering, E. T. J. *Science* **2003**, *301*, 349–352.
- (18) Mohammed, O. F.; Pines, D.; Dreyer, J.; Pines, E.; Nibbering, E. T. J. *Science* **2005**, *310*, 83–86.
- (19) Westlake, B. C.; Brennaman, M. K.; Concepcion, J. J.; Paul, J. J.; Bettis, S. E.; Hampton, S. D.; Miller, S. A.; Lebedeva, N. V.; Forbes, M. D. E.; Moran, A. M.; et al. *Proc. Natl. Acad. Sci. U.S.A.* **2011**, *108*, 8554–8558.
- (20) Shaw, G. B.; Brown, C. L.; Papanikolas, J. M. *J. Phys. Chem. A* **2002**, *106*, 1483–1495.
- (21) Habeeb, M. M. *App. Spec. Rev.* **1997**, *32*, 103–140.
- (22) Concepcion, J. J.; Brennaman, M. K.; Deyton, J. R.; Lebedeva, N. V.; Forbes, M. D. E.; Papanikolas, J. M.; Meyer, T. J. *J. Am. Chem. Soc.* **2007**, *129*, 6968–6969.
- (23) Shank, C. V.; Dienes, A.; Trozzolo, A. M.; Myer, J. A. *Appl. Phys. Lett.* **1970**, *16*, 405–407.
- (24) Choudhury, S. D.; Pal, H. *J. Phys. Chem. B* **2009**, *113*, 6736–6744.
- (25) Choudhury, S. D.; Nath, S.; Pal, H. *J. Phys. Chem. B* **2008**, *112*, 7748–7753.
- (26) Moriya, T. *Bull. Chem. Soc. Jpn.* **1988**, *61*, 753–759.
- (27) Moriya, T. *Bull. Chem. Soc. Jpn.* **1988**, *61*, 1873–1886.
- (28) Schulman, S. G.; Rosenberg, L. S. *J. Phys. Chem.* **1979**, *83*, 447–451.